Relativistic spectral random-phase approximation in finite nuclei

John F. Dawson
Department of Physics, University of New Hampshire, Durham, New Hamphire 03824

R. J. Furnstahl
Department of Physics and Astronomy, University of Maryland, College Park, Maryland 20742
(Received 26 March 1990)

A relativistic random-phase approximation (RPA) description of discrete excitations in closed-shell nuclei is presented using a spectral approach, with emphasis on the nature and importance of self-consistency. A functional derivation of self-consistent RPA equations is given, based on a nonrelativistic formalism, and its generalization is discussed. Vacuum polarization is neglected, but consistency demands configuration spaces that include both particle-hole pairs and pairs formed from occupied states and negative-energy states, which ensures current conservation and the decoupling of the spurious state. Results in the Walecka (σ-ω) model for various isoscalar states in ^{12}C, ^{16}O, and ^{40}Ca, are given, including electron scattering form factors.

I. INTRODUCTION

With nuclear experimental facilities moving toward higher momentum transfers [e.g., Continuous Electron Beam Accelerator Facility (CEBAF)] and extreme conditions [e.g, Relativistic Heavy Ion Collider (RHIC)], new insight into the treatment of relativistic many-body systems of hadrons will be required. To draw definite and reliable conclusions about such systems, theoretical calculations must maintain general physical properties, such as covariance, gauge invariance, and causality. One way to do this is to use a relativistic quantum field theory based on mesons and baryons, which is referred to as quantum hadrodynamics (QHD).[1] In this paper, we present QHD calculations of discrete excitations in closed-shell nuclei, with emphasis on the nature of self-consistency in this particular problem and its role in preserving basic physical principles.[2-4]

One of the compelling aspects of QHD is the richness of physics at the mean-field level. Mean-field approximations to QHD provide a relativistic saturation mechanism of nuclear matter and naturally predict the spin-orbit interaction.[1] Self-consistency at this level ensures that the description of nuclear matter is covariant[5] and thermodynamically consistent.[6] Mean-field (Hartree) calculations of finite nuclei successfully describe ground-state rms radii, charge densities, neutron densities, quadrupole deformations, and spin-orbit splittings[7,8] and provide densities for calculations of elastic proton-nucleus scattering. The predictions of spin observables, using a simple impulse approximation in conjunction with Hartree densities, have been remarkably successful.[9] We would like to describe excitations as the *consistent* linear response of mean-field ground states.

Since relativistic mean-field models have been most successful in describing bulk isoscalar properties of nuclei, it is reasonable to expect that isoscalar, low-lying collective excitations of natural parity will be well described using a time-dependent mean-field picture. In such a picture, all of the nucleons can contribute coherently to the excitation through the mean meson fields, which are themselves determined by time-dependent fluctuations in the scalar and vector nucleon densities. By linearizing the time-dependent Hartree equations, we obtain the relativistic random-phase approximation (RPA). Here we present a relativistic RPA description of discrete collective excitations, applying a spectra approach. These calculations provide consistent relativistic nuclear structure input for new studies of the inelastic scattering of polarized protons and other probes. (Similar calculations using nonspectral methods have been reported recently.[10])

An alternate and more general route to the RPA is to formulate the linear response in terms of a Bethe-Salpeter equation for particle-hole scattering.[11] Two questions of consistency arise in this context. First, we must specify both an approximation to the fermion self-energy and to the Bethe-Salpeter kernel. In general, they cannot be chosen independently and still maintain conservation laws. As can be shown from the linearization described above, the consistent linear response of a Hartree ground state is given diagrammatically by the sum of ring contributions to the polarization propagator. We will demonstrate this relationship in the context of a functional approach to the RPA equations, which may be generalized to higher-order approximations.

A second question of consistency arises when a mean-field approximation to the self-energy is used. Two types of relativistic mean-field approximations, which we shall refer to as the relativistic Hartree approximation (RHA) and the mean-field theory (MFT), can be applied to calculations of finite nuclei. The RHA is the full one-nucleon-loop approximation, which incorporates the effects of the mean fields on the states in the Dirac sea and so includes vacuum contributions to the energy and source densities.[1] The MFT is Walecka's original high-density approximation to nuclear matter; it includes self-consistent contributions to the energy and the source densities from only

 ©1990 The American Physical Society

the occupied positive-energy nucleons.[1] Here we are interested in the linear response to an MFT ground state and how it is formulated.

One might think that the linear response of the MFT would involve only conventional positive-energy particle-hole configurations, as in the nonrelativistic RPA. However, this neglects the fact that a complete relativistic single-particle basis includes positive- *and* negative-energy solutions. Recent studies of nuclear currents in relativistic mean-field theories have emphasized the contribution to the MFT elastic response from the mixing of positive- and negative-energy single-particle solutions.[12] This mixing is responsible for the quenching of the isoscalar part of the magnetic moment of nuclei. We show here that it is also essential for the MFT inelastic response, and quantify its importance.

The RPA equations can be solved using either "spectral" or "nonspectral" methods. In the spectral approach, the lowest-order polarization insertion (nucleon ring) is built from Hartree propagators written in a spectral representation. That is, each Green's function is written as a discretized and truncated sum over eigenfunctions of the nucleon Dirac equation. In the nonspectral approach, the ring is rewritten in terms of a sum over occupied (positive-energy) states and a nonspectral Green's function, which is constructed at each energy from linearly independent solutions of the Dirac equation.

The poles of the full particle-hole (polarization) propagator occur at the collective excitation energies of the nucleus and the residues are proportional to the corresponding transition amplitudes.[11] With the equation in spectral form, one can equate residues at the poles to derive RPA matrix equations of the same form as in the nonrelativistic RPA. These matrices are diagonalized to obtain discrete energies and RPA amplitudes in the discretized basis. In contrast, in the nonspectral approach one evaluates the response function at a given (complex) frequency by solving the integral equation directly (by iteration or matrix inversion). One then searches for poles near the real axis (for discrete states) and extracts the residues to determine transition densities. In principle, at least, these two methods should give the same answers for discrete excitations.

In this work, we apply spectral methods. This approach lets us clearly show that the negative-energy states (which have been omitted from previous spectral RPA calculations[13]) are required to obtain a consistent result; while quantifying their importance. In particular, we show that configurations with negative-energy states are needed to realize the spurious state as a decoupled zero-energy state and to maintain current conservation. Our calculations also provide a useful check of nonspectral calculations.[10]

We restrict our discussion to isoscalar excitations, although extending the formalism given here to isovector excitations is straightforward. Since ground-state (bulk) properties in the Hartree approximation are mostly determined by the isoscalar mesons, only the isoscalar particle-hole interaction is significantly constrained by a consistent treatment of the excited states. As argued above, we may expect a successful description of collective isoscalar excitations in the RPA, but a good description of isovector excitations does not necessarily follow. In fact, other authors have found that the isovector particle-hole spectrum is not realistically described in the Hartree-RPA approximation,[14] and suggest that a more sophisticated treatment is required (e.g., Hartree-Fock).

The outline of the paper is as follows. In Sec. II we discuss self-consistency and conserving approximations, and outline a functional approach to consistent RPA equations. In Sec. III we present the spectral realization of these equations and discuss their solution. Selected results for ^{12}C, ^{16}O, and ^{40}Ca are given in Sec. IV, with illustrations of current conservation and the decoupling of the spurious state. Section V contains some final discussion and a summary.

II. SELF-CONSISTENCY AND CONSERVING APPROXIMATIONS

Self-consistent approximations to the many-body properties of strongly interacting nonrelativistic systems have been extensively studied.[15,16] But can we make truncations of a (strongly interacting) relativistic quantum field theory that are self-consistent in some sense? In theories that can be treated perturbatively, one can work consistently to a given order in the coupling constant. This is not a useful prescription for strong-coupling theories, which we consider here, where nonperturbative approximations are essential. Another approach is to work to a given order in a different expansion parameter, such as $\hbar$ in a loop expansion, which is nonperturbative in the mean meson fields. However, the ordinary loop expansion has not proven useful (beyond one loop) for quantum hadrodynamics.[17] As an alternative, we will focus on a prescription for nonrelativistic self-consistent approximations.[15,16]

We begin by specifying what we hope to achieve by working self-consistently. We cannot solve the full field theory so we must make approximations, and strong couplings imply that diagrams at every order in the couplings must be included in any useful approximation. But, to the greatest extent possible, we want to maintain the constraints imposed by symmetries (Ward identities) and basic physical principles (e.g., causality). (This is a principal motivation for the QHD approach to the relativistic many-body problem.[1]) Self-consistency can help to define physically reasonable truncations that maintain desirable features of the full theory. In addition, given an approximation to the ground state (or equilibrium state) of a relativistic system, we want to know how to consistently describe the linear response so that symmetries are preserved. Self-consistency can ensure that the same correlations that are important in determining the ground state (in some approximation) determine the behavior of small deviations from equilibrium.[15]

These considerations are particularly important here because self-consistency plays a greater role in relativistic models of nuclei than in nonrelativistic descriptions. For example, the single-particle wave functions for nonrelativistic Hartree-Fock in nuclear matter are simply Pauli

spinors times plane waves. In relativistic Hartree in nuclear matter, the wave functions are plane waves multiplied by four-component spinors, which must be determined self-consistently. In practice, it will usually be necessary to relax self-consistency to make a calculation tractable. This can be particularly dangerous in the relativistic many-body problem because of the characteristic large mass scales (e.g., the meson mean fields) and so we need to be aware of the sensitivity of observables to violations of self-consistency. While in nonrelativistic nuclear physics the penalty is often small and more convenient approximations can be used, substantial and essential errors can be made in the relativistic approach. The isoscalar "magnetic moment problem" provides a characteristic example. (See Ref. 8 for details and other references.)

To gain insight into defining useful truncations of relativistic field theories, we can look at schemes for deriving nonrelativistic self-consistent approximations. The many-body problem in this case involves fermions or bosons interacting via *instantaneous* two-body potentials. Baym and Kadanoff showed how to generate a class of self-consistent approximations to self-energies and correlation functions that conserve particle number, energy, and momentum, and which are thermodynamically consistent.[15,16] Furthermore, spurious modes due to symmetries broken by the self-energy appear as zero-energy poles in the linear response function. These are called conserving approximations. The approach they developed provides guidelines for selecting the partial summation of diagrams that determine an approximation to the self-energy and linear response functions.

It is natural to try to apply the same approximations or their analogs to relativistic models. However, generalizing the Baym-Kadanoff formalism to a relativistic quantum field theory to address these questions is not straightforward because of new aspects of the relativistic problem, such as dynamical mesons, retardation, and ultraviolet divergences. In a fully interacting field theory, we must deal with Dyson's equations for the nucleon *and* meson propagators, as well as the infinite hierarchy of equations for the vertices. As a result, not all nonrelativistic approximations remain conserving when made relativistic.[2] Nevertheless, the mean-field approximation can be formulated by adapting the nonrelativistic framework, and we do so below.

First, we present a functional version of the Baym formalism schematically; more details can be found in Ref. 18. One introduces Φ_2, the set of two-particle irreducible Feynman graphs, considered as a functional of the one-body propagator G: $\Phi_2=\Phi_2[G]$. A conserving approximation starts with an approximation to Φ_2, which can be made diagrammatically by specifying a subset of the graphs. Then the proper self-energy is determined by a functional derivative:

$$\Sigma=\Sigma[G]=\mp\frac{\delta\Phi_2}{\delta G}\ , \tag{2.1}$$

and the propagator is determined self-consistently through Dyson's equation:

$$G=G_0+G_0\Sigma[G]G\ . \tag{2.2}$$

(The signs are for bosons/fermions.) Finally, the correlation function L satisfies a Bethe-Salpeter equation whose kernel is found from $\Sigma[G]$:

$$L=\mp GG\mp GG\frac{\delta\Sigma}{\delta G}L\ . \tag{2.3}$$

Examples of symmetry-conserving approximations in the nonrelativistic problem include the Hartree, Hartree-Fock, and Brueckner-Hartree-Fock approximations.

If a symmetry of the Hamiltonian is associated with a unitary transformation U, so that

$$[U,H]=0\ , \tag{2.4}$$

and the propagator is transformed $\bar{G}$ according to

$$\bar{G}=UGU^{\dagger}\ , \tag{2.5}$$

then

$$\Phi_2[\bar{G}]=\Phi_2[G]\text{ and }\Sigma[\bar{G}]=\bar{\Sigma}[G]\ . \tag{2.6}$$

If $G=\bar{G}$, then $[U,\Sigma]=0$ and U is a self-consistent symmetry, which is maintained as Dyson's equation is iterated. An example is gauge invariance that leads to current conservation. If $G\neq\bar{G}$, then $\bar{\Sigma}[G]\neq\Sigma[G]$, and U is a broken symmetry. However, as demonstrated in Ref. 18, the construction from Φ_2 implies that the particle-hole Green's function L has a pole at zero energy. An example of a broken symmetry is translational invariance, which is broken by the mean-field propagator for a finite nucleus. The zero-energy pole in this case is the isoscalar 1^- spurious state.

III. RELATIVISTIC SPECTRA RPA

A. Consistent RPA equations

In adapting the conserving-approximation formalism to the relativistic mean-field approximation, lowest-order meson propagators and vertices replace the potential, but the rest of the development goes through basically unchanged. However, this works only because of the simplicity of the Hartree approximation. Generalizing to higher approximations requires fundamental changes, because the interaction is mediated by dynamical mesons. As a result, Φ_2 will become a functional of the full meson propagators and vertices. Such functionals are introduced in the effective action formalism of Refs. 19 and 20, but a generalized conserving-approximation formalism does not yet exist.

In the nonrelativistic problem, the simplest subset of graphs for Φ_2 leads to the Hartree approximation and to the RPA. It is also the basis for our relativistic treatment of the MFT as a conserving approximation. Specifically, the relativistic mean-field Φ_2 is

$$\Phi_2[G_H]=-\frac{i}{2}g_s^2\int d(1)d(2)\mathrm{Tr}[G_H(1,1^+)]\times\Delta_0(1-2)\mathrm{Tr}[G_H(2,2^+)]-\frac{i}{2}g_v^2\int d(1)d(2)\mathrm{Tr}[\gamma_\mu(1,1^+)]\times D_0^{\mu\nu}(1-2)\mathrm{Tr}[\gamma_\nu(2,2^+)]\ , \tag{3.1}$$

where G_H is the self-consistent Hartree propagator, the 1^+ notation indicates the time-ordering prescription for single-fermion closed loops (see Ref. 1), and Δ_0 and $D_0^{\mu\nu}$ are the noninteracting scalar and vector meson propagators.[1] The trace is over Dirac indices and isospin and we use the shorthand

$$\int d(1)\equiv\int d^3x_1dt_1\ . \tag{3.2}$$

Note that Lorentz covariance dictates the use of the full interaction in (3.1) (i.e., γ^μ and not just γ^0). This is because we need to consider arbitrary variations of G_H, even though in the spherical ground state the three-vector contribution (the meson field $\mathbf{V}$) vanishes.

The mean-field self-energy is defined by a functional derivative:

$$\begin{aligned}\Sigma^H(1,2)&=\frac{\delta\Phi_2[G_H]}{\delta G_H(1,2)}\\&=\delta^4(1-2)\left[-ig_s^2\int d(3)\Delta_0(1-3)\mathrm{Tr}[G_H(3,3^+)]-\gamma_\mu ig_v^2\int d(3)D_0^{\mu\nu}(1-3)\mathrm{Tr}[\gamma_\nu G_H(3,3^+)]\right]\\&\equiv\delta^4(1-2)[\Sigma_s(1)-\gamma_\mu\Sigma_v^\mu(1)]\ ,\end{aligned} \tag{3.3}$$

where the Dirac indices are implicit. Then the Dyson equation for the nucleon propagator is

$$G_H(1,2)=G_0(1,2)+\int d(3)d(4)G_0(1,3)\Sigma^H(3,4)G_H(4,2)\ , \tag{3.4}$$

where G_0 is the noninteracting Green's function. By operating with G_0^{-1} and using the definitions above, we find

$$\{\gamma_\mu[i\partial^\mu+\Sigma_v^\mu(x)]-[M+\Sigma_s(x)]\}G_H(x,x')=\delta^4(x-x')\ . \tag{3.5}$$

Equation (3.5) can be solved by expanding the Green's function G_H in a standard spectral representation

$$\begin{aligned}G_H(1,2)&=\int\frac{d\omega}{2\pi}G_H(\mathbf{r}_1,\mathbf{r}_2;\omega)e^{-i\omega(t_1-t_2)}\ ,\\G_H(\mathbf{r}_1,\mathbf{r}_2;\omega)&=\sum_\alpha\psi_\alpha(\mathbf{r}_1)\bar\psi_\alpha(\mathbf{r}_2)G_\alpha^H(\omega)\ ,\end{aligned} \tag{3.6}$$

where $\psi_\alpha(\mathbf{r})$ is a *complete* set of eigenstates with eigenvalues ϵ_α, including positive and negative eigenvalues, and

$$\begin{aligned}G_\alpha^H(\omega)&=\frac{\theta(-\epsilon_\alpha)}{\omega-\epsilon_\alpha-i\eta}+\frac{\theta(\epsilon_\alpha-\epsilon_F)}{\omega-\epsilon_\alpha+i\eta}+\frac{\theta(\epsilon_F-\epsilon_\alpha)\theta(\epsilon_\alpha)}{\omega-\epsilon_\alpha-i\eta}\\&=G_\alpha^F(\omega)+G_\alpha^D(\omega)\ ,\end{aligned} \tag{3.7}$$

where ϵ_F is the Fermi energy. In the first two lines, we have separated the negative-energy $[\theta(-\epsilon_\alpha)]$, unoccupied positive-energy $[\theta(\epsilon_\alpha-\epsilon_F)]$, and filled positive-energy $[\theta(\epsilon_F-\epsilon_\alpha)\theta(\epsilon_\alpha)]$ states. The third line is another useful grouping of these terms. The Feynman (G^F) and density-dependent (G^D) parts of the Hartree Green's function are defined by

$$\begin{aligned}G_\alpha^F(\omega)&=\frac{\theta(\epsilon_\alpha)}{\omega-\epsilon_\alpha+i\eta}+\frac{\theta(-\epsilon_\alpha)}{\omega-\epsilon_\alpha-i\eta}\ ,\\G_\alpha^D(\omega)&=2\pi i\delta(\omega-\epsilon_\alpha)\theta(\epsilon_F-\epsilon_\alpha)\theta(\epsilon_\alpha)\ .\end{aligned} \tag{3.8}$$

As it stands, (3.6) leads to a divergent self-energy when substituted into Eq. (3.3) because of contributions from the occupied Dirac sea, so we must renormalize. If we follow this path, we define the RHA. [Note, however, that we would have to extend the framework implied by Eq. (3.1) to deal with the counterterms.] The usual MFT prescription is to keep only contributions to the self-energy (or in the RPA rings) from terms that are explicitly density dependent.[7] Equivalently, one normal orders operator products in the vacuum of the self-consistent problem. However, simply eliminating $G_\alpha^F(\omega)$ is not an acceptable solution within the conserving-approximation framework because $G_H(1,2)$ would not then satisfy Eq. (3.5): The positive-energy solutions alone are not a complete set.

However, we can make an alternative ansatz for G_H, which we will designate $\tilde G_H$, which accomplishes the MFT prescription by shifting the negative-energy poles to the lower-half plane, as if the Dirac sea were empty. In particular,

$$\tilde G_\alpha^H(\omega)=\frac{\theta(-\epsilon_\alpha)}{\omega-\epsilon_\alpha+i\eta}+\frac{\theta(\epsilon_\alpha-\epsilon_F)}{\omega-\epsilon_\alpha+i\eta}+\frac{\theta(\epsilon_F-\epsilon_\alpha)\theta(\epsilon_\alpha)}{\omega-\epsilon_\alpha-i\eta}\ . \tag{3.9}$$

This new propagator is also constructed from a complete set of solutions to the Dirac equation, and satisfies Dyson's equation. (We also modify G_0 in the same manner.) The integrals in the self-energies pick up only the positive-energy occupied state poles, as desired. Thus, we reproduce the normal-ordering prescription of the MFT using the analytic structure of $\tilde G_H$. Furthermore, we maintain the same spectral content: The modified propagators will give us the same ground-state and excited-state observables (energies and densities) as obtained through the MFT prescription.

Substituting $\tilde G_H$ into Eq. (3.5) yields the familiar Dirac eigenvalue equation for the ground-state MFT,[8]

$$\{-i\boldsymbol{\alpha}\cdot\nabla+\beta[M-g_s\phi_0(\mathbf{r})]+g_v[V_0(\mathbf{r})-\boldsymbol{\alpha}\cdot\mathbf{V}(\mathbf{r})]\}\psi_\alpha(\mathbf{r})=\epsilon_\alpha\psi_\alpha(\mathbf{r}) , \tag{3.10}$$

where $g_s\phi_0\equiv-\Sigma_s$ is the scalar mean field and $g_v V_0\equiv-\Sigma_v^\mu$ is the vector mean field [with $V^\mu=(V_0,\mathbf{V})$]. There are solutions for both positive and negative energies. The self-energies are evaluated using $\tilde{G}_H$ in Eq. (3.3), which results in the usual MFT meson equations.[7]

Finally, we can apply Eq. (2.3) to write the Bethe-Salpeter equation for the propagator L, defined as

$$L(1,2;1',2')=-\{\langle\Psi_0|T[\hat{\psi}(1)\hat{\bar{\psi}}(1')\hat{\psi}(2)\hat{\bar{\psi}}(2')]|\Psi_0\rangle-\langle\Psi_0|T[\hat{\psi}(1)\hat{\bar{\psi}}(1')]|\Psi_0\rangle\langle\Psi_0|T[\hat{\psi}(2)\hat{\bar{\psi}}(2')]|\Psi_0\rangle\} . \tag{3.11}$$

The consistent MFT/RPA kernel follows from

$$\frac{\delta\Sigma^H(1,2)}{\delta G_H(3,4)}=\delta^4(1-2)\delta^4(3-4)[-ig_s^2\Delta_0(1-3)-\gamma_\mu^{(1)}ig_v^2D_0^{\mu\nu}(1-3)\gamma_\nu^{(3)}]$$

$$\equiv i\delta^4(1-2)\delta^4(3-4)V(1,3) , \tag{3.12}$$

which implies that L is defined by a ring sum, as expected. The last line in (3.12) defines the particle-hole interaction V.

To study particle-hole excitations, it is sufficient to consider L with $1'=1^+$ and $2'=2^+$, which defines the polarization Green's function Π:[11]

$$i\Pi_{abcd}(1,2)=\langle\Psi_0|T[\hat{\bar{\psi}}_a(1)\hat{\psi}_b(1)\hat{\bar{\psi}}_c(2)\hat{\psi}_d(2)]|\Psi_0\rangle-\langle\Psi_0|\hat{\bar{\psi}}_a(1)\hat{\psi}_b(1)|\Psi_0\rangle\langle\Psi_0|\hat{\bar{\psi}}_c(2)\hat{\psi}_d(2)|\Psi_0\rangle$$

$$=i\int\frac{d\omega}{2\pi}\Pi(\mathbf{r}_1,\mathbf{r}_2;\omega)e^{-i\omega(t_1-t_2)} . \tag{3.13}$$

For later convenience we have indicated Dirac spinor indices explicitly (they will usually be suppressed). The Fourier transform of the polarization function has simple poles at the discrete particle-hole excitations of the system, with residues given by the particle-hole amplitudes. Because of the simple form of the kernel (3.12), we can consider an equation for Π instead of the full L. (This is not possible beyond the Hartree/RPA approximation.)

Then the integral equation for the modified MFT/RPA polarization, $\tilde{\Pi}_{\rm RPA}$, is given by [see Eq. (2.3)]

$$\tilde{\Pi}_{\rm RPA}(1,2)=\tilde{\Pi}_{\rm MFT}(1,2)+\int d(3)d(4)\tilde{\Pi}_{\rm MFT}(1,3)V(3,4)\tilde{\Pi}_{\rm RPA}(4,2) , \tag{3.14}$$

where $V(1,2)$ is given by Eq. (3.12) and $\tilde{\Pi}_{\rm MFT}$, the MFT noninteracting polarization propagator, is constructed using $\tilde{G}_H$,

$$i\tilde{\Pi}_{\rm MFT}(\mathbf{r}_1,\mathbf{r}_2;\omega)=\int\frac{d\omega'}{2\pi}\tilde{G}_H(\mathbf{r}_1,\mathbf{r}_2;\omega+\omega')\tilde{G}_H(\mathbf{r}_2,\mathbf{r}_1;\omega')$$

$$=\sum_{\alpha,\beta}\bar{\psi}_\beta(\mathbf{r}_1)\psi_\alpha(\mathbf{r}_1)\bar{\psi}_\alpha(\mathbf{r}_2)\psi_\beta(\mathbf{r}_2)\int\frac{d\omega'}{2\pi}\tilde{G}_\alpha^H(\omega+\omega')\tilde{G}_\beta^H(\omega') . \tag{3.15}$$

Applying Eq. (3.9), we obtain

$$\tilde{\Pi}_{\rm MFT}(\mathbf{r}_1,\mathbf{r}_2;\omega)=\sum_{\alpha\beta;\alpha'\beta'}\bar{\psi}_\beta(\mathbf{r}_1)\psi_\alpha(\mathbf{r}_1)\tilde{\Pi}^{\rm MFT}_{\alpha\beta;\alpha'\beta'}(\omega)\bar{\psi}_{\alpha'}(\mathbf{r}_2)\psi_{\beta'}(\mathbf{r}_2) ,$$

$$\tilde{\Pi}^{\rm MFT}_{\alpha\beta;\alpha'\beta'}(\omega)=\delta_{\alpha,\alpha'}\delta_{\beta,\beta'}\left[\frac{N_{\alpha\beta}}{\omega-\epsilon_{\alpha\beta}+i\eta}-\frac{N_{\beta\alpha}}{\omega+\epsilon_{\beta\alpha}-i\eta}\right] , \tag{3.16}$$

$$N_{\alpha\beta}\equiv p_\alpha h_\beta+v_\alpha h_\beta ,$$

where $\epsilon_{\alpha\beta}\equiv\epsilon_\alpha-\epsilon_\beta$, and p_α, h_α, and v_α are the particle, positive-energy hole, and negative-energy state regions defined by

$$p_\alpha=\theta(\epsilon_\alpha-\epsilon_F) , \quad h_\alpha=\theta(\epsilon_F-\epsilon_\alpha)\theta(\epsilon_\alpha) , \quad v_\alpha=\theta(-\epsilon_\alpha) . \tag{3.17}$$

Thus, we find contributions from particle-hole pairs and from pairs made of negative-energy states and positive-energy holes.

If we had used G_H instead of $\tilde{G}_H$ in Eq. (3.15), we would have found

$$G_\alpha^H(\omega+\omega')G_\beta^H(\omega')=G_\alpha^F(\omega+\omega')G_\beta^F(\omega')+G_\alpha^F(\omega+\omega')G_\beta^D(\omega')+G_\alpha^D(\omega+\omega')G_\beta^F(\omega')+G_\alpha^D(\omega+\omega')G_\beta^D(\omega') . \tag{3.18}$$

The usual MFT prescription of including only explicitly density-dependent contributions would require the $G_\alpha^FG_\beta^F$ term in (3.18) to be removed by hand. From this point of view, we remove the full vacuum polarization, leaving minus the part of the vacuum response that is Pauli blocked in the nuclear medium.[3] The resulting polarization propagator $\Pi_{\rm MFT}$ would have the same spectral content as $\tilde{\Pi}_{\rm MFT}$ (which is what we care about), but the poles involving negative-energy states would be in the opposite half-plane.

Expanding $\tilde{\Pi}_{\rm RPA}$ in the particle-hole basis,

$$\tilde{\Pi}_{\mathrm{RPA}}(\mathbf{r}_1,\mathbf{r}_2;\omega)=\sum_{\alpha\beta;\alpha'\beta'}\bar{\psi}_\beta(\mathbf{r}_1)\psi_\alpha(\mathbf{r}_1)\tilde{\Pi}^{\mathrm{RPA}}_{\alpha\beta;\alpha'\beta'}(\omega)\bar{\psi}_{\alpha'}(\mathbf{r}_2)\psi_{\beta'}(\mathbf{r}_2)\ , \tag{3.19}$$

we get from (3.14),

$$\tilde{\Pi}^{\mathrm{RPA}}(\omega)=\tilde{\Pi}^{\mathrm{MFT}}(\omega)+\tilde{\Pi}^{\mathrm{MFT}}(\omega)K(\omega)\tilde{\Pi}^{\mathrm{RPA}}(\omega)\ . \tag{3.20}$$

We have defined

$$K_{\alpha\beta;\alpha'\beta'}(\omega)\equiv\langle\alpha,\beta'|V(\omega)|\beta,\alpha'\rangle\ , \tag{3.21}$$

and the matrix elements by

$$\langle\alpha,\beta|V(\omega)|\alpha',\beta'\rangle=\int d^3\mathbf{r}_1\int d^3\mathbf{r}_2[\psi^\dagger_\beta(\mathbf{r}_1)\psi^\dagger_\alpha(\mathbf{r}_2)V_\omega(r_{12})\psi_{\alpha'}(\mathbf{r}_1)\psi_{\beta'}(\mathbf{r}_2)]\ , \tag{3.22}$$

$$V_\omega(r_{12})=-\beta_1\beta_2\frac{g_s^2}{4\pi}\frac{e^{-\tilde{m}_s r_{12}}}{r_{12}}+(1-\boldsymbol{\alpha}_1\cdot\boldsymbol{\alpha}_2)\frac{g_v^2}{4\pi}\frac{e^{-\tilde{m}_v r_{12}}}{r_{12}}\ , \tag{3.23}$$

where $r_{12}\equiv|\mathbf{r}_1-\mathbf{r}_2|$, and $\tilde{m}^2_{s,v}\equiv m^2_{s,v}-\omega^2$ incorporates the effects of retardation. Because the interaction V_ω is used in matrix elements of four-component Dirac spinors, its form is deceptively simple. If the interaction were to be reduced for use with conventional two-component spinors, it would become an infinite series of terms with complicated radial and spin dependencies (e.g., tensor, spin-orbit, etc.). We note once again that it is important to keep the full interaction for consistency.

Equation (3.20) can be reduced to an RPA matrix equation for discrete states by introducing a Lehman representation and equating residues at excited-state poles.[13] We give an alternative derivation here, based on the discussion in Ref. 11. Within the extended particle-hole space, we can define an inverse for the polarization matrices such that $\Pi^{-1}\Pi=I$, where

$$I_{\alpha\beta;\alpha'\beta'}=\delta_{\alpha,\alpha'}\delta_{\beta,\beta'}(N_{\alpha\beta}+N_{\beta\alpha})\ . \tag{3.24}$$

Then from (3.20), we find

$$\tilde{\Pi}^{\mathrm{RPA}}(\omega)^{-1}=\tilde{\Pi}^{\mathrm{MFT}}(\omega)^{-1}-K(\omega)\ , \tag{3.25}$$

where

$$\tilde{\Pi}^{\mathrm{MFT}}_{\alpha\beta;\alpha'\beta'}(\omega)^{-1}=\delta_{\alpha,\alpha'}\delta_{\beta,\beta'}(\omega-\epsilon_{\alpha\beta})(N_{\alpha\beta}-N_{\beta\alpha})\ . \tag{3.26}$$

We invert (3.25) by considering the eigenvalue problem,

$$\sum_{\alpha'\beta'}[\tilde{\Pi}^{\mathrm{MFT}}_{\alpha\beta;\alpha'\beta'}(\omega_n)^{-1}-K_{\alpha\beta;\alpha'\beta'}(\omega_n)]C^{(n)}_{\alpha'\beta'}=0\ . \tag{3.27}$$

The states in (3.27) are restricted to the particle-hole basis defined by the identity matrix (3.24). We can write the eigenvectors $C^{(n)}_{\alpha\beta}$ more conventionally as

$$C^{(n)}_{\alpha\beta}=N_{\alpha\beta}X^{(n)}_{\alpha\beta}+N_{\beta\alpha}Y^{(n)}_{\beta\alpha}\ . \tag{3.28}$$

Substitution of (3.28) into (3.27) gives the relativistic spectral RPA equations,

$$\sum_{\alpha'\beta'}\begin{bmatrix}A_{\alpha\beta;\alpha'\beta'} & B_{\alpha\beta;\alpha'\beta'}\\ B_{\alpha\beta;\alpha'\beta'} & A_{\alpha\beta;\alpha'\beta'}\end{bmatrix}\begin{bmatrix}X^{(n)}_{\alpha'\beta'}\\ Y_{\alpha'\beta'}\end{bmatrix}=\omega_n N_{\alpha\beta}\begin{bmatrix}X^{(n)}_{\alpha\beta}\\ -Y^{(n)}_{\alpha\beta}\end{bmatrix}\ , \tag{3.29}$$

where

$$A_{\alpha\beta;\alpha'\beta'}(\omega_n)=N_{\alpha\beta}[\delta_{\alpha,\alpha'}\delta_{\beta,\beta'}\epsilon_{\alpha\beta}+K_{\alpha\beta;\alpha'\beta'}(\omega_n)]N_{\alpha'\beta'}\ , \tag{3.30}$$

$$B_{\alpha\beta;\alpha'\beta'}(\omega_n)=N_{\alpha\beta}[K_{\alpha\beta;\beta'\alpha'}(\omega_n)]N_{\alpha'\beta'}\ .$$

These are the equations we actually solve. If we had followed the usual MFT/RPA prescription, we would have obtained the same equations, although the labels of X and Y for negative-energy configurations would be switched. The observables of interest (excitation energies and transition densities) are the same.

In these equations, ω_n is the energy difference between the excited (positive-energy) collective particle-hole excitation and the ground state. For the states we consider, it is much smaller than the meson masses, and so retardation is negligible for the matrix elements in (3.23). (This has been verified numerically; see below.) If we neglect retardation, properties of solutions to the nonrelativistic RPA carry over directly. The solutions of the RPA equations (3.29) satisfy the orthogonality condition

$$\sum_{\alpha\beta}N_{\alpha\beta}(X^{(n')*}_{\alpha\beta},Y^{(n')*}_{\alpha\beta})\begin{bmatrix}X^{(n)}_{\alpha\beta}\\ -Y^{(n)}_{\alpha\beta}\end{bmatrix}=\lambda_n\delta_{n,n'}\ , \tag{3.31}$$

and completeness relation

$$N_{\alpha'\beta'}N_{\alpha\beta}\sum_n\lambda_n\begin{bmatrix}X^{(n)}_{\alpha'\beta'}\\ X^{(n)}_{\alpha'\beta'}\end{bmatrix}(X^{(n)*}_{\alpha\beta},-Y^{(n)*}_{\alpha\beta})=N_{\alpha\beta}\delta_{\alpha,\alpha'}\delta_{\beta,\beta'}1\ , \tag{3.32}$$

where

$$\lambda_n=1,\text{for } n>0\ ;$$
$$=-1,\text{ for } n<0\ .$$

We may now use (3.25) and (3.27) to find a solution to

$$\tilde{\Pi}^{\mathrm{RPA}}_{\alpha\beta,\alpha'\beta'}(\omega)=\sum_{n>0}\left[\frac{C^{(n)}_{\alpha\beta}C^{(n)*}_{\alpha'\beta'}}{\omega-\omega_n+i\eta}-\frac{C^{(n)}_{\beta'\alpha'}C^{(n)*}_{\beta\alpha}}{\omega+\omega_n-i\eta}\right]\ . \tag{3.33}$$

Thus the solutions of (3.29) are indeed the poles of the polarization operator.

B. Form factors and current conservation

To calculate inelastic electron scattering form factors, we follow the discussion in Ref. 1 and introduce an effective electromagnetic current operator, to be used with relativistic Hartree wave functions:

$$\hat{J}^{\mu}(x) \doteq \bar{\psi}(x)\gamma^{\mu}Q\psi(x) + \frac{1}{2M}\partial_{\nu}(\bar{\psi}(x)\lambda\sigma^{\mu\nu}\psi(x)) , \tag{3.34}$$

where the field operators are in the Heisenberg representation, and

$$\begin{aligned} &Q \equiv \tfrac{1}{2}(1+\tau_3) , \\ &\lambda \equiv \lambda_p \tfrac{1}{2}(1+\tau_3) + \lambda_n \tfrac{1}{2}(1-\tau_3) \end{aligned} \tag{3.35}$$

are the charge and anomalous magnetic moment operators. The momentum dependence of the single-nucleon form factors is folded into the nuclear form factors at the end of the calculation. The idea is that the nuclear structure in mean-field models is dominated by neutral mesons while the single-nucleon structure, at least within QHD, is predominately determined by charged mesons, which are beyond the scope of the Hartree/RPA. Thus, it is reasonable to decouple these contributions.

Matrix elements of the current between the closed-shell ground state and the RPA excited states (labeled by n) define the transition currents. In terms of the RPA amplitudes, transition current densities are given by

$$\begin{aligned} J^{\mu(n)}(\mathbf{r}) &= \tfrac{1}{2}\sum_{\alpha\beta} C^{(n)*}_{\alpha\beta}(\bar{\psi}_{\alpha}(\mathbf{r})\gamma^{\mu}\psi_{\beta}(\mathbf{r})) \\ &= \tfrac{1}{2}\sum_{\alpha\beta} N_{\alpha\beta}[X^{(n)*}_{\alpha\beta}\bar{\psi}_{\alpha}(\mathbf{r})\gamma^{\mu}\psi_{\beta}(\mathbf{r}) \\ &\quad + Y^{(n)*}_{\alpha\beta}\bar{\psi}_{\beta}(\mathbf{r})\gamma^{\mu}\psi_{\alpha}(\mathbf{r})] , \end{aligned} \tag{3.36}$$

for the Dirac part of the isoscalar current, with analogous expressions for the anomalous current. With

$$J^{\mu(n)}(\mathbf{r}) \equiv (\rho^{(n)}(\mathbf{r}), \mathbf{J}^{(n)}(\mathbf{r})) ,$$

the multipole charge and current densities for transitions between the ground state (with $J=0$) and the RPA excited state (with $J=J_n$) are defined by[21]

$$\begin{aligned} M^{(n)}_{JM}(q) &\equiv \int d^3x\, j_J(qx) Y_{JM}(\Omega)\rho^{(n)}(\mathbf{x}) \\ &\equiv \langle J_n M_n 00|JM\rangle M^{(n)}_J(q)/\sqrt{2J+1} , \\ T^{(n)}_{JLM}(q) &\equiv \int d^3x\, j_L(qx)\mathbf{Y}_{JLM}(\Omega)\cdot\mathbf{J}^{(n)}(\mathbf{x}) \\ &\equiv \langle J_n M_n 00|JM\rangle T^{(n)}_{JL}(q)/\sqrt{2J+1} , \end{aligned} \tag{3.37}$$

where j_L is a spherical Bessel function, and $\mathbf{Y}_{JLM}(\Omega)$ are the vector spherical harmonics.[22] The longitudinal and transverse form factors are given in terms of the reduced matrix elements, $M^{(n)}_J(q)$ and $T^{(n)}_{JL}(q)$,

$$\begin{aligned} F^2_L(q) &= |M^{(n)}_J(q)|^2 , \\ F^2_T(q) &= |T^{\mathrm{el}(n)}_J(q)|^2 + |T^{\mathrm{mag}(n)}_J(q)|^2 , \end{aligned} \tag{3.38}$$

where the electric and magnetic reduced matrix elements are given by

$$\begin{aligned} T^{\mathrm{el}(n)}_J(q) &= i\left[-\left[\frac{J}{2J+1}\right]^{1/2} T^{(n)}_{J,J+1}(q) \right. \\ &\quad \left. + \left[\frac{J+1}{2J+1}\right]^{1/2} T^{(n)}_{J,J-1}(q)\right] , \\ T^{\mathrm{mag}(n)}_J(q) &= T^{(n)}_{J,J}(q) . \end{aligned} \tag{3.39}$$

Explicit expressions for reduced matrix elements of relativistic multipole operators have been given elsewhere.[13,10]

The current conservation relation for $\tilde{\Pi}_{\mathrm{RPA}}(1,2)$ can be derived most easily by considering an equivalent formulation of conserving approximations,[15,16] in which we consider the propagator $G^U(1,1')$ in the presence of a nonlocal source $U(2,2')$. If we can determine G^U with a given approximation for the self-energy (which also depends on U), the consistent particle-hole correlation function L is given by

$$L(1,2;1',2') = \left.\frac{\delta G^U(1,1')}{\delta U(2',2)}\right|_{U=0} . \tag{3.40}$$

This is the same L as derived from Φ_2.[16] As before, Π is obtained by setting $1'=1^+$ and $2'=2^+$.

Now consider the equations for $\tilde{G}^U_H$ in the presence of an external source U:

$$\begin{aligned} &\int d(1'')\{[i\gamma_{\mu}\partial^{\mu}_{1''} - M - \Sigma^H_U(1'')]\delta^4(1-1'') - U(1,1'')\}\tilde{G}^U_H(1'',1') = \delta^4(1-1') , \\ &\int d(1'')\tilde{G}^U_H(1,1'')\{\delta^4(1''-1')[-i\gamma_{\mu}\partial^{\mu}_{1''} - M - \Sigma^H_U(1'')] - U(1'',1')\} = \delta^4(1-1') , \end{aligned} \tag{3.41}$$

where the derivatives in the second equation act to the left. If we subtract these equations, set $1'=1^+$, take the Dirac trace in the spinor indices associated with 1, and then take the functional derivative with respect to $U(2,2')$ and set $U=0$, we obtain a current conservation relation for $L(1,2;1,2')$. It has singular pieces [proportional to $\delta^4(1-2)$ and $\delta^4(1'-2')$] coming from the time derivative of the time-ordering theta functions in L [see Eq. (3.11)] and the equal-time commutation relations for the fermion fields. We avoid these terms by considering separate coordinates 1 and 2 ($1\neq 2$), with $2'=2^+$, and find

$$\{\gamma_{\mu}\}_{ab}\partial^{\mu}_1 \tilde{\Pi}^{\mathrm{RPA}}_{abcd}(1,2) = 0 , \quad 1\neq 2 . \tag{3.42}$$

(One can show an analogous relation in the other variable.) The terms involving the self-energies cancel au-

tomatically *even if they are not consistent,* but only because the self-energies are local in space-time in the mean-field approximation. Thus, current conservation in the RPA requires completeness [in Eq. (3.41)], but not consistency of the interaction.

After taking the Fourier transform in time, Eq. (3.42) is satisfied for all ω, and in particular, for $\omega=\omega_n$. In this case, we obtain the current conservation relation for the transition current [using Eqs. (3.36) and (3.33)]:

$$i\omega_n\rho^{(n)}(\mathbf{r})+\nabla\cdot\mathbf{J}^{(n)}(\mathbf{r})=0\ . \tag{3.43}$$

Equation (3.43) implies that the longitudinal part of the multipole current, $L_J^{(n)}(q)$, is proportional to the charge density. That is,

$$qL_J^{(n)}(q)+\omega_n M_J^{(n)}(q)=0\ , \tag{3.44}$$

where

$$L_J^{(n)}(q)=i\left[\left[\frac{J+1}{2J+1}\right]^{1/2}T_{J,J+1}^{(n)}(q) + \left[\frac{J}{2J+1}\right]^{1/2}T_{J,J-1}^{(n)}(q)\right]\ . \tag{3.45}$$

This relation is tested (and verified) numerically below. One can also prove Eq. (3.43) directly using the matrix RPA equations and completeness of the single-particle basis.[10]

C. Calculational details

We make an angular momentum and isospin reduction of (3.28) and (3.30), and reduce (3.29) to a (generalized) eigenvalue problem for states of total J and T, exactly as in the nonrelativistic case. To evaluate the matrix elements, we expand the Yukawa functions in spherical harmonics and Bessel functions. The problem is then reduced to Slater integrals and standard angular momentum coupling coefficients and reduced matrix elements. (See Ref. 13 for formulas and further details.) The RPA eigenvalues and eigenvectors are obtained as the result of standard matrix inversions.

As we have stressed, the single-particle spectrum in the Hartree approximation, namely the eigenvalues of the Dirac equation that describes nucleon motion, includes both positive- and negative-energy states. For spherical nuclei, there are a relatively small number of weakly bound positive-energy states and then a positive-energy continuum starting at the nucleon mass. In contrast, the strong scalar and vector potentials add in the effective negative-energy potential, leading to a large number (several hundred) of bound negative-energy states. For example, there are eight bound $s_{1/2}$ negative-energy levels in ^{16}O for the mean-field model of Ref. 7.

We approximate the exact $\tilde{G}_H(\mathbf{r}_1,\mathbf{r}_2)$ by discretizing the continuum solutions and truncating the sums to a finite number of terms. The positive and negative continua are discretized by imposing boundary conditions on the single-particle wave functions at a radius R several times the nuclear radius. Various choices for the boundary conditions can be made, including those used in bag models. In practice, the most convenient choice is to set either the upper or lower (but not both) components of the Dirac spinors to zero at R and normalize to one inside the sphere. This generates an orthonormal basis that is approximately complete. The discretization can be tested by varying R and the type of boundary conditions. For the calculations presented here, all results are independent of the boundary conditions once the sums have converged (i.e., with a large enough configuration space).

All calculations in this paper are in the σ-ω model with parameters from Ref. 7 (except as noted below for ^{40}Ca). The ground-state parameters completely determine both the single-particle basis and the unperturbed energies, as well as the isoscalar particle-hole interaction. (In nonrelativistic calculations with phenomenological potentials, the unperturbed energies are generally taken from experiment or otherwise adjusted to get good fits to experimental data.)

IV. RESULTS

In this section, we present calculations of selected low-lying collective $T=0$ states in ^{12}C, ^{16}O, and ^{40}Ca, with particular emphasis on the role of negative-energy basis states in spectral RPA calculations. We use the mean-field parameter set from Ref. 7: $g_s^2=109.6$, $m_s=520$ MeV, $g_v^2=190.4$, and $m_v=783$ MeV. This parametrization provides a reasonable description of the ground-state properties of closed-shell nuclei (binding energies, rms radii, charge densities), although the surface energy and compressibility are somewhat too large. We note that mean-field models that include nonlinear self-couplings for the scalar mesons (ϕ^3 and ϕ^4 terms in the Lagrangian) provide superior descriptions of ground-state properties, particularly for deformed nuclei.[8] However, applying these models to an RPA calculation of excited states is technically much more difficult than for the linear model, because the scalar-meson propagator no longer has a simple Yukawa form.

The discretized single-particle basis is obtained by applying boundary conditions at a radius several times the nuclear radius (12 fm in ^{16}O), as described above. A large configuration space is necessary to ensure that traces of the spurious 1^- are eliminated from physical 1^- states; we used up to 200 configurations in our calculations. This included positive-energy states up to several hundred MeV's in the continuum and the entire bound negative-energy spectrum of states.

With a large enough space, energies and transition densities are stable with respect to the size of the basis and independent of the boundary conditions. We illustrate this conclusion in Fig. 1, where we plot the position of the spurious $T=0$, $J^\pi=1^-$ state and two low-lying collective states in ^{16}O as a function of the total number of configurations, with both positive-energy and negative-energy configurations included (dashed lines). As seen in the figure, a large number of configurations (over 150) are needed to achieve convergence. The results with different values of the cutoff were qualitatively similar, although the number of configurations needed for stability in-

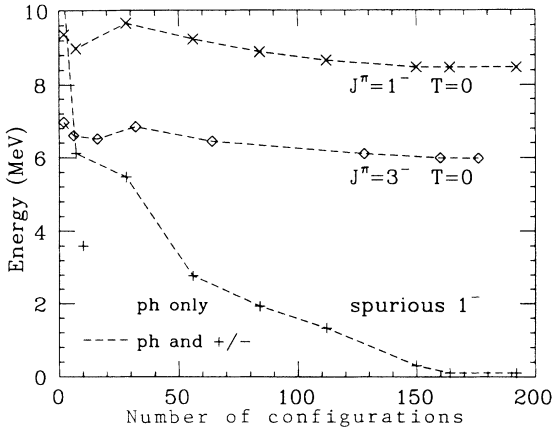

FIG. 1. Energy of the spurious state and other low-lying isoscalar states in ^{16}O in a spectral RPA calculation, as a function of the size of the configuration space.

creased with the cutoff value, and small values of the cutoff (below 10 fm) tend to significantly distort bound-state wave functions.

Figure 1 demonstrates that the spurious 1^- state appears as a decoupled zero-energy state in the RPA spectrum, if a sufficiently complete configuration space is used. The contribution from configurations with negative-energy states is essential to achieve this result. The dotted line shows the energy of the spurious state when only positive-energy particle-hole configurations are included. In this case, the energy drops rapidly with larger spaces but soon becomes imaginary and never approaches zero. We also note that the contribution to the interaction from the three-vector omega exchange is needed to decouple the spurious state.

We show in Fig. 2 the low-lying $T=0$ negative-parity states in ^{16}O, along with certain experimental levels that we might hope to describe as particle-hole excitations. For clarity, only the lowest states of each J are shown. The first column shows the unperturbed levels from the ground-state calculation. The second column is the RPA spectrum when only particle-hole configurations are included and the third column is the full RPA spectrum, including all states. Retardation effects are negligible for these low-lying states, because the excitation energies are much smaller than the meson masses. This was verified by iterating the RPA equations with frequency-dependent masses for the mesons.

Overall, the spectrum in the third column is very reasonable for a fully self-consistent RPA calculation, especially in view of the large cancellations inherent in relativistic models. It is also evident from the second column that configurations with negative-energy states play a significant role in determining the energy levels, particularly for the very collective states. To test the RPA wave functions, we consider inelastic electron scattering to these states.

First, we tested the conservation of transition currents as a function of the number and type of configurations employed. In Fig. 3, we plot the ratio (with appropriate factors of q and ω) of the matrix elements of the transition charge and longitudinal current densities for the $T=0$, $J^\pi=3^-$ state in ^{16}O for $q=1$ fm^{-1}, which typifies our results. This ratio should be equal to 1 for all values of q, and we see that it does approach that value if enough configurations are used. (The number of configurations needed to converge to one increases with the momentum transfer.) The dotted line shows that current is *not conserved* if only the particle-hole configurations are used. Thus, the negative-energy states are necessary for a correct description of the transition densities.

Calculated electron scattering form factors for selected low-lying collective natural parity states in ^{16}O, ^{12}C, and ^{40}Ca are compared with data in Figs. 4–11. In each of

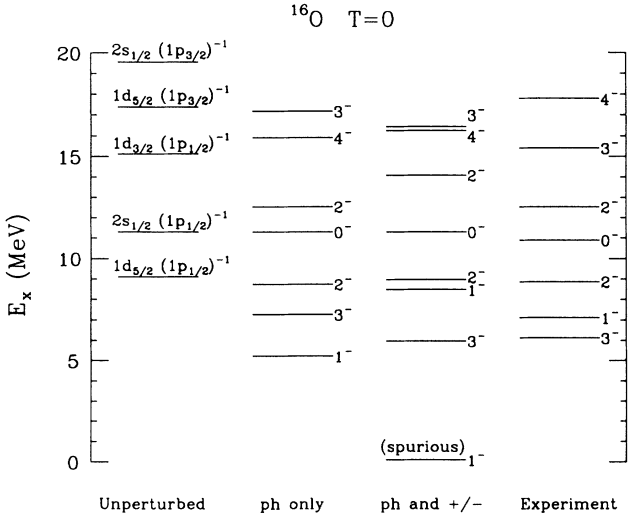

FIG. 2. Energy levels of selected low-lying states in ^{16}O in a spectral RPA calculation.

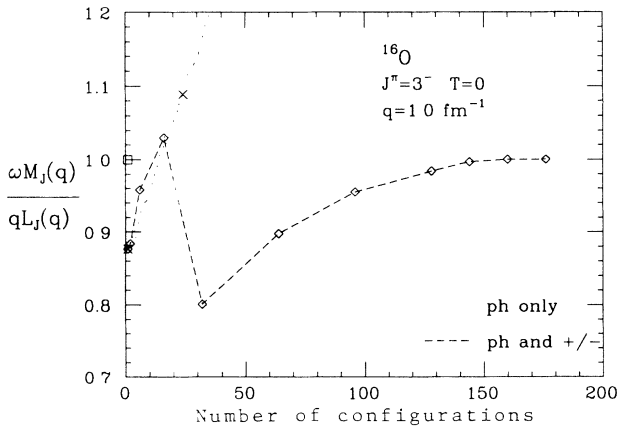

FIG. 3. Ratio of transition charge to longitudinal current densities for the low-lying isoscalar 3^- state in ^{16}O, as a function of the configuration space size. The densities are evaluated at $q=1.0$ fm^{-1}.

these figures, the solid line is the form factor for the uncorrelated (Hartree) particle-hole state that is the dominant configuration in the RPA wave function, and the dot-dashed line is the full RPA calculation. Comparisons of these two curves provide a measure of the collectivity of the states. The form-factor calculations include a center-of-mass correction and single-nucleon form factors, as described in Ref. 13. These form factors have also been calculated using a nonspectral RPA approach.[10] The nonspectral results are essentially identical to those presented here.

The longitudinal form factor for the 2^+ state at 4.44 MeV in ^{12}C is shown in Fig. 4. This state shows significant collectivity in the RPA calculations, leading to good agreement with the experimental strength. The RPA energy for this state is about 4 MeV; the energy is almost 2 MeV higher if negative-energy configurations are excluded. The transverse electric form factor for this state is shown in Fig. 5. Current conservation constrains the form factor at low momentum transfer, but while the RPA result is quenched with respect to the single-particle result at intermediate q, it still lies well above the data. In these calculations, the carbon ground state is simply modeled as a closed $1p_{3/2}$ shell.

The 1^- state at 7.1 MeV in ^{16}O shown in Fig. 6 is particularly interesting because it provides a sensitive test of self-consistency. Only a fully self-consistent calculation will completely eliminate spurious center-of-mass contributions to the wave function for this state. A large amount of configuration mixing is required to remove the $J=1$ character of the longitudinal form factor at low q, and we note that the RPA calculations succeed here, but again, only with negative-energy configurations and the three-vector omega interaction included. The momentum dependence of the experimental data is well reproduced by the RPA calculation, but the strength is a factor of 2 too low. The transverse electric form factor is compared to data in Fig. 7. The calculation of the 6.13 MeV 3^- state in ^{16}O shown in Fig. 8 predicts significant collectivity, as found experimentally. (The predicted energy is 6.0 MeV.) Again, the momentum dependence is quite reasonable, but the strength is about $\frac{2}{3}$ the experimental form factor. About the same result is obtained in nonrelativistic self-consistent RPA calculations.[23]

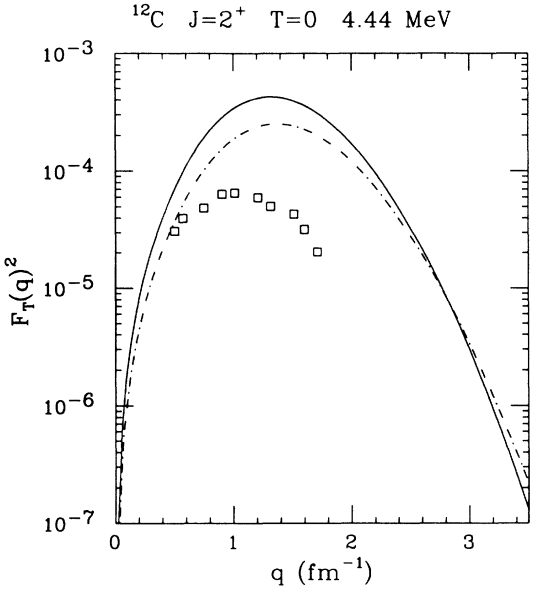

FIG. 5. Transverse form factor for the 4.4 MeV isoscalar 2^+ state in ^{12}C. The RPA curve (dot-dashed) is compared to an unperturbed $1p_{1/2}(1p_{3/2})^{-1}$ pair (solid) and to data.

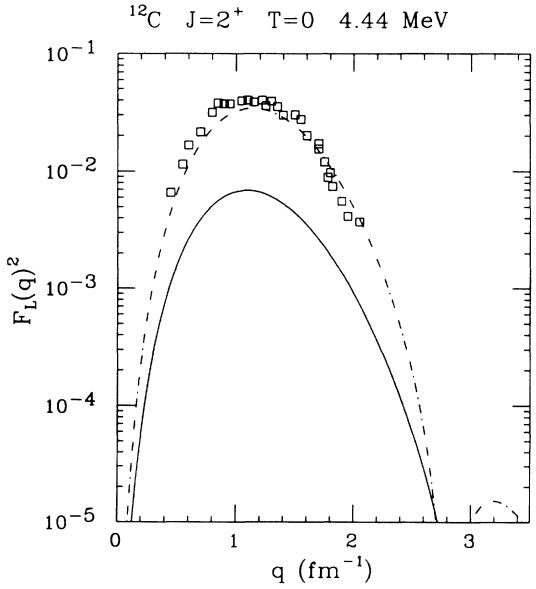

FIG. 4. Longitudinal form factor for the 4.4 MeV isoscalar 2^+ state in ^{12}C. The RPA curve (dot-dashed) is compared to an unperturbed $1p_{1/2}(1p_{3/2})^{-1}$ pair (solid) and to data.

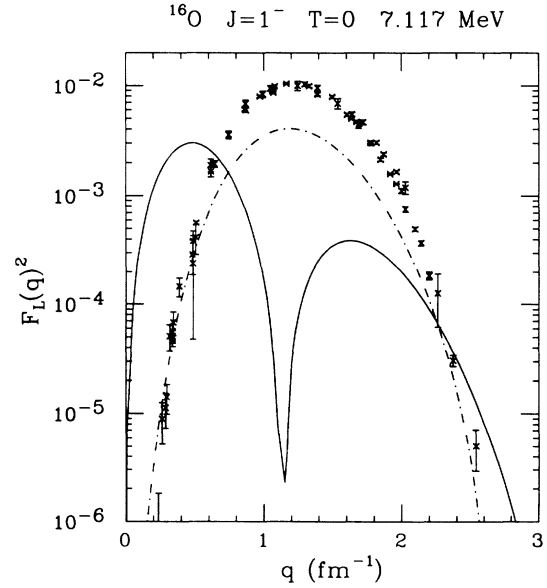

FIG. 6. Longitudinal form factor for the 7.1 MeV isoscalar 1^- state in ^{16}O. The RPA curve (dot-dashed) is compared to an unperturbed $1s_{1/2}(1p_{1/2})^{-1}$ pair (solid) and to data (Ref. 25).

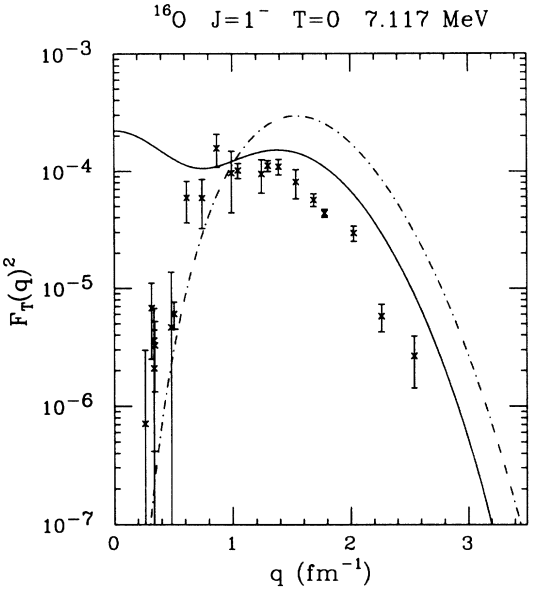

FIG. 7. Transverse form factor for the 7.1 MeV isoscalar 1^- state in ^{16}O. The RPA curve (dot-dashed) is compared to an unperturbed $1s_{1/2}(1p_{1/2})^{-1}$ pair (solid) and to data (Ref. 25).

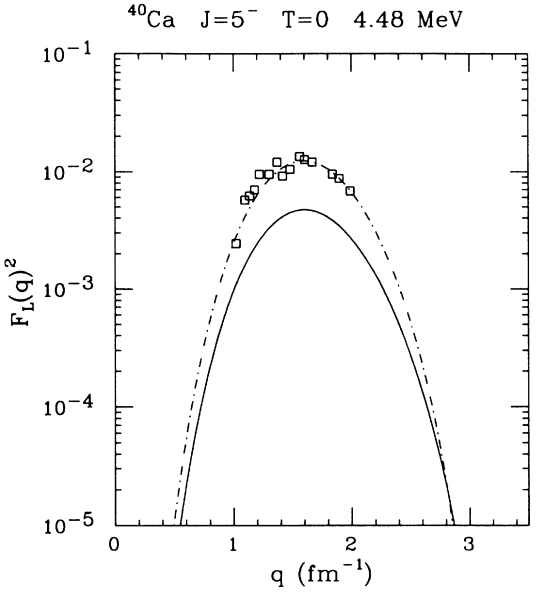

FIG. 9. Longitudinal form factor for the 4.5 MeV isoscalar 5^- state in ^{40}Ca. The RPA curve (dot-dashed) is compared to an unperturbed $1f_{7/2}(1d_{3/2})^{-1}$ pair (solid) and to data.

In ^{40}Ca, we find the low-lying 4.48 MeV 5^- state at 4.0 MeV in the RPA with a longitudinal form factor in good agreement with experiment (Fig. 9). However, the collective 3.76 MeV 3^- state appears at an *imaginary* energy with the parameter set of Ref. 7. Imaginary frequencies in the RPA indicate instabilities of the Hartee ground state.[24] A calculation using a truncated basis reveals that this instability is driven by the particle-hole response from high in the continuum. If we truncate the particle-hole space at several "shells" ($\sim$50 MeV in the continuum), the energy of the 3^- is real (about 2 MeV) and the form factor is reasonable (dot-dashed curve in Fig. 10). The energy and collectivity of this state are very sensitive to details of the interaction and can be made real in the full calculation by slightly adjusting the parameters of the model. For example, when ^{40}Ca is calculated with the scalar-meson coupling squared reduced by 2% and the scalar-meson mass adjusted to reproduce the same nu-

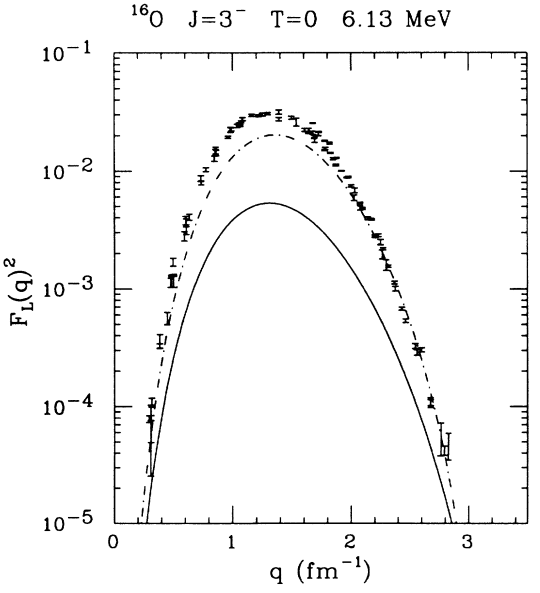

FIG. 8. Longitudinal form factor for the 6.1 MeV isoscalar 3^- state in ^{16}O. The RPA curve (dot-dashed) is compared to an unperturbed $1d_{5/2}(1p_{1/2})^{-1}$ pair (solid) and to data (Ref. 25).

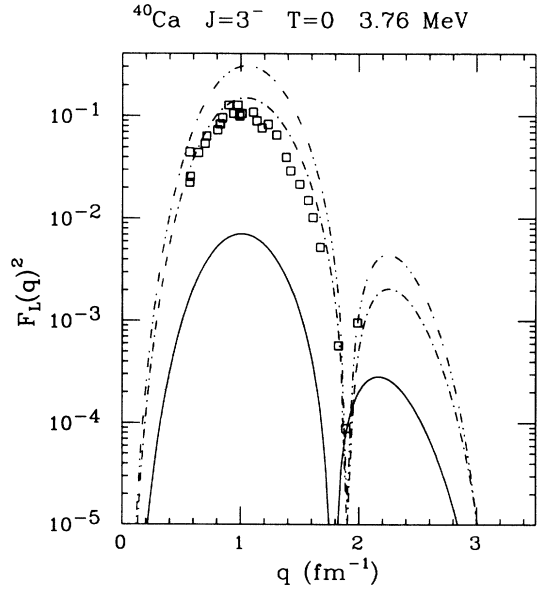

FIG. 10. Longitudinal form factor for the 3.8 MeV isoscalar 3^- state in ^{40}Ca. (See text for explanation of curves).

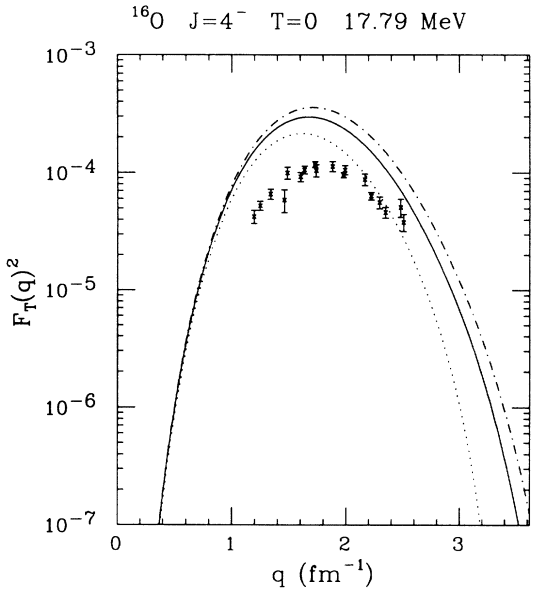

FIG. 11. Transverse form factor for the 17.8 MeV isoscalar 4^- state in ^{16}O. The RPA curve (dot-dashed) is compared to an unperturbed $1d_{5/2}(1p_{3/2})^{-1}$ pair (solid) and to a nonrelativistic reduction (dots). Data are from Ref. 26.

clear matter saturation properties as in Ref. 7, the 3^- state is found near 1 MeV and the form factor is given by the double-dot-dashed curve. Instabilities of the mean-field theory ground state have also been observed in other contexts. (See Ref. 24 and references cited therein.)

Finally, we consider the unnatural parity transitions, for which the nuclear response is mediated solely by the three-vector part of the ω meson interaction. Here the character of the results (and problems) is very similar to those found in calculations of elastic magnetic scattering.[8] In particular, the calculated electron scattering form factors for the unnatural parity states do not describe the experimental data unless significant quenching factors are applied. A typical example is the 4^- state, shown in Fig. 11. The RPA curve reproduces the experimental momentum dependence but requires a quenching factor of about 0.3.

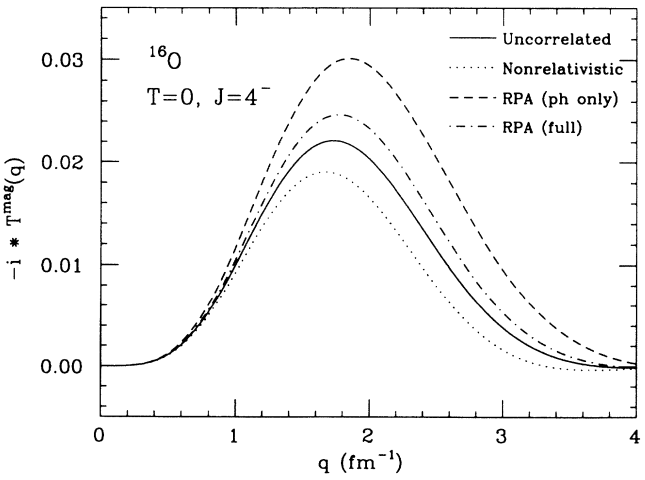

FIG. 12. Dirac current in momentum space for the 17.8 MeV isoscalar 4^- state in ^{16}O. (See text for explanation of curves).

To clarify this result, the transition current (Dirac part only) for the lowest 4^- state in ^{16}O is shown in Fig. 12, with curves for the uncorrelated $1d_{5/2}(1p_{3/2})^{-1}$ particle-hole pair (solid), a nonrelativistic reduction[12] (dots), RPA with only particle-hole configurations (dashed), and the full spectral RPA (dot-dashed) calculations. The M/M^* enhancement of the valence current with respect to the nonrelativistic current is further enhanced at finite q in the RPA by the particle-hole response. (Note the dramatic enhancement that occurs when only particle-hole configurations are included.) This result is consistent with calculations of the linear response in nuclear matter[24] and the elastic response in finite nuclei.[12] The discrepancy between the predictions and the data can be reduced but not eliminated by including vacuum polarization corrections.[28]

V. SUMMARY

In this paper, we presented consistent relativistic RPA calculations of discrete excitations in closed-shell nuclei, using a spectral approach. We have shown how the mean-field theory (MFT) of the nuclear ground state, which omits contributions to the self-energy from the Dirac sea, and its linear response (RPA ring sum) can be accommodated in the nonrelativistic framework of conserving approximations. However, this adaptation requires that the negative-energy poles in the conventional Hartree propagator be shifted to the lower-half plane. With this change, the equations that follow from the standard MFT/RPA prescription of keeping only (explicitly) density-dependent contributions to the self-energies and RPA rings are duplicated, while the conserving properties of the relativistic RPA follow directly.

We find that contributions from configurations built from holes (occupied positive-energy states) and negative-energy states are essential for a complete and convergent description of the low-lying states in the RPA, in practice as well as in principle. In particular, they are needed to preserve current conservation and the decoupling of the spurious translational state, and contribute to the collectivity of excited states. When these configurations are included, we find a reasonable description of the isoscalar collective states (natural parity). In contrast, the electron scattering form factors for unnatural parity states consistently overpredict the data, just as is found in relativistic mean-field calculations of elastic magnetic electron scattering.[12]

The spectral techniques used here rely on a discretization and truncation of the continuum. Care must be taken that the response is not distorted by these approximations. As we have shown, large configuration spaces are needed to obtain stable, converged results, which implies that our approach is inefficient and limited. We note, however, that consistent and accurate spectral calculations with much smaller configuration spaces (and much

less computational effort) are possible by using "optimized" single-particle basis functions, based on b splines.[27]

As an alternative, one can turn to a nonspectral approach,[10] which offers some advantages. For example, the negative-energy contributions to the response are included automatically and both positive- and negative-energy continuua are treated exactly. Thus, this method is well suited to describing a wide range of inelastic nuclear response, from discrete states through the giant resonance region to the quasielastic region. Nonspectral methods have recently been used to include vacuum polarization corrections to the calculation of low-lying excited states, using a local density approximation.[28] It is interesting to note that much less collectivity is predicted in these RHA/RPA calculations than in the MFT/RPA calculations, despite a reasonable description of ground-state properties.

Which is the more appropriate mean-field description? While the MFT is (usually) more successful phenomenologically, one could argue that the RHA is a more consistent and complete mean-field treatment. In terms of linear response, the RPA ring contributions in the MFT can be identified as the usual particle-hole response minus the Pauli-blocked piece of the vacuum response. Keeping only part of the vacuum response seems unnatural at best; a theoretically complete treatment at the mean-field level would include the effects of the mean-fields on the Dirac sea nucleons, as well as on the occupied positive-energy states.

On the other hand, while the RHA may be conceptually more complete than the MFT, the treatment of the vacuum might not approximate physical reality very well. After all, theoretical consistency does not always imply correct physics. Indeed, the role of vacuum corrections in hadronic field theories is a subject of controversy because of arguments that the composite nature of nucleons is not handled correctly.[29] For example, the authors of two recent papers argue that the physics of the loop corrections is wrong because it is not consistent with the $1/N_c$ expansion of QCD.[30] It is argued that the vacuum physics must be modified if a hadronic field theory is to describe nature, and should be treated separately from "valence" nucleon physics (due to positive-energy occupied states). However, as we have seen, even the apparent separation of valence and vacuum physics in the ground-state MFT still requires considering Dirac sea states in the RPA.

What about consistent relativistic calculations of linear response beyond the mean-field level? Blunden and McCorquodale have applied relativistic Hartree-Fock (HF) wave functions to spectral RPA calculations, including both direct and exchange matrix elements of the interaction (and neglecting retardation).[14] Their approach is basically a relativistic generalization of standard nonrelativistic HF/RPA. Their calculations provide insight into the nature and importance of the isovector interaction and the role of exchange contributions in determining the energy spectrum. However, they worked with a comparatively small configuration space, and only positive-energy basis states were included, so these are not fully consistent calculations. In fact, a fully consistent formulation of relativistic HF/RPA is not known at present.

Finally, we need to know if vacuum effects can be modified or separated out in the relativistic many-body problem beyond the mean-field level, without sacrificing basic physical principles. To address these questions, extensions of the functional approach to generating conserving approximations to a full relativistic field theory treatment, based on the generalized effective action formalism of Refs. 19 and 20, are being considered. Whether good truncations of hadronic field theories beyond the mean-field level are possible is not obvious, however, unlike the nonrelativistic case. This is an important problem for future study.

ACKNOWLEDGMENTS

One of us (J.F.D.) would like to thank C. J. Horowitz and B. D. Serot for hospitality at the nuclear theory center at Indiana University Cyclotron Facility (IUCF), where much of this work was performed. This work was supported by the U.S. Department of Energy under contracts DE-FG05-87ER-40322 and DE-FG02-88ER-40410.

[1]B. D. Serot and J. D. Walecka, *Advances in Nuclear Physics* (Plenum, New York, 1986), Vol. 16.

[2]R. J. Furnstahl, in *Relativistic Nuclear Many-Body Physics,* edited by B. C. Clark, R. J. Perry, and J. P. Vary (World Scientific, Singapore, 1989).

[3]R. J. Furnstahl, in *Spin Observables of Nuclear Probes,* edited by C. Horowitz, C. D. Goodman, and G. E. Walker (Plenum, New York, 1988), and references therein.

[4]Some of the results presented here have been discussed previously at conferences (see Refs. 2 and 3).

[5]R. J. Furnstahl and B. D. Serot, Nucl. Phys. **A468**, 539 (1987).

[6]R. J. Furnstahl and B. D. Serot, Phys. Rev. C **41**, 262 (1990).

[7]C. J. Horowitz and B. D. Serot, Nucl. Phys. **A368**, 503 (1981).

[8]R. J. Furnstahl and C. E. Price, Phys. Rev. C **40**, 1398 (1989).

[9]L. G. Arnold, B. C. Clark, R. L. Mercer, and P. Schwandt, Phys. Rev. C **23**, 1949 (1981), and references cited.

[10]J. R. Shepard, E. Rost, and J. A. McNeil, Phys. Rev. C **40**, 2320 (1989).

[11]A. L. Fetter and J. D. Walecka, *Quantum Theory of Many-Particle Systems* (McGraw-Hill, New York, 1971).

[12]R. J. Furnstahl, Phys. Rev. C **38**, 370 (1988).

[13]R. J. Furnstahl, Ph.D. thesis, Stanford University, 1985; Phys. Lett. **152B**, 313 (1985).

[14]P. Blunden and P. McCorquodale, Phys. Rev. C **38**, 1861 (1988).

[15]G. Baym and L. P. Kadanoff, Phys. Rev. **124**, 287 (1961).

[16]G. Baym, Phys. Rev. **127**, 1391 (1962); Phys. Lett. **1**, 242 (1962).

[17]R. J. Furnstahl, R. J. Perry, and B. D. Serot, Phys. Rev. C **40**, 321 (1989).

[18]J. P. Blaizot and G. Ripka, *Quantum Theory of Finite Systems* (MIT, Cambridge, MA, 1986).
[19]H. D. Dahmen and G. Jona-Lasinio, Nuovo Cimento **52A**, 807 (1967).
[20]R. E. Norton and J. M. Cornwall, Ann. Phys. (N.Y.) **91**, 106 (1975).
[21]T. W. Donnelly and J. D. Walecka, Annu. Rev. Nucl. Sci. **25**, 329 (1975).
[22]A. R. Edmonds, *Angular Momentum in Quantum Mechanics* (Princeton University, Princeton, NJ, 1960).
[23]P. Ring and P. Schuck, *The Nuclear Many-Body Problem* (Springer-Verlag, New York, 1980).
[24]R. J. Furnstahl and C. J. Horowitz, Nucl. Phys. **A485**, 632 (1988).
[25]T. N. Buti, Ph.D. thesis, Massachusetts Institute of Technology, 1984.
[26]C. E. Hyde-Wright, Ph.D. thesis, Massachusetts Institute of Technology, 1984.
[27]J. A. McNeil, R. J. Furnstahl, E. Rost, and J. R. Shepard, Phys. Rev. C **40**, 399 (1989).
[28]J. Piekarewicz, Indiana University Report IU/NTC 89-18 1989.
[29]S. L. Brodsky, Comments Nucl. Part. Phys. **12**, 213 (1984); J. W. Negele, *ibid.* **14**, 303 (1985); I. Zahed, Phys. Rev. C **37**, 409 (1988).
[30]T. D. Cohen, Phys. Rev. Lett. **62**, 3027 (1989); E. Kiritsis and R. Seki, *ibid.* **63**, 953 (1989).